Solar Phys (2014) 289:4701–4709
DOI 10.1007/s11207-014-0587-6

Cosmogenic Isotope Variability During the Maunder Minimum: Normal 11-year Cycles Are Expected

S.V. Poluianov · I.G. Usoskin · G.A. Kovaltsov

Received: 9 December 2013 / Accepted: 29 July 2014 / Published online: 14 August 2014

Abstract The amplitude of the 11-year cycle measured in the cosmogenic isotope ^{10}Be during the Maunder Minimum is comparable to that during the recent epoch of high solar activity. Because of the virtual absence of the cyclic variability of sunspot activity during the Maunder Minimum this seemingly contradicts an intuitive expectation that lower activity would result in smaller solar-cycle variations in cosmogenic radio-isotope data, or in none, leading to confusing and misleading conclusions. It is shown here that large 11-year solar cycles in cosmogenic data observed during periods of suppressed sunspot activity do not necessarily imply strong heliospheric fields. Normal-amplitude cycles in the cosmogenic radio-isotopes observed during the Maunder Minimum are consistent with theoretical expectations because of the nonlinear relation between solar activity and isotope production. Thus, cosmogenic-isotope data provide a good tool to study solar-cycle variability even during grand minima of solar activity.

Keywords Cosmic rays · Maunder minimum · Solar cycle

1. Introduction

While the dominant feature of solar activity, traditionally quantified in sunspot numbers, is the 11-year solar cycle, the Sun sometimes enters specific periods of greatly suppressed

S.V. Poluianov · I.G. Usoskin (✉)
Department of Physics, University of Oulu, 90014 Oulu, Finland
e-mail: Ilya.Usoskin@oulu.fi

G.A. Kovaltsov
Ioffe Physical-Technical Institute, 194021 St. Petersburg, Russia

I.G. Usoskin
Sodankylä Geophysical Observatory (Oulu Unit), University of Oulu, 90014 Oulu, Finland

sunspot activity, called grand minima. The most recent of such grand minima was the Maunder Minimum in the second half of the 17th century, when there were virtually no spots on the Sun, so that the 11-year cycle almost vanished during that time. This is in great contrast to the modern period of high solar activity when the sunspot number spanned from almost zero during the solar-cycle minimum to more than 100 during the solar-maximum years. On the other hand, we know that, despite the absence of sunspots, the solar cycle was still observable in geomagnetic and heliospheric indicators during the Maunder Minimum (Beer, Tobias, and Weiss, 1998; Cliver, Boriakoff, and Bounar, 1998). However, both the overall level and the amplitude of the 11-year cycle in heliospheric activity were greatly reduced during the Maunder Minimum.

Cosmogenic radio-isotopes are produced mainly by galactic cosmic rays in the Earth's atmosphere and form the only quantitative proxy for solar activity on the long-term scale, and its verification with the direct data over the last centuries forms a basis for solar/heliospheric magnetic-activity reconstructions in the past (Beer, McCracken, and von Steiger, 2012). The two commonly used cosmogenic isotopes are ^{10}Be, usually measured in polar ice cores, and ^{14}C, measured in tree rings. Both isotopes are produced by cosmic rays in the atmosphere and are subject to different terrestrial transport processes. Since cosmic rays are modulated by solar magnetic activity in the heliosphere, their variability serves as a proxy for the latter, forming the basis for the method. Therefore, its verification with the direct data over the last few centuries forms the basis for the solar-activity reconstructions in the past (Usoskin, 2013).

Radiocarbon ^{14}C takes part in the global carbon cycle, which leads to significant attenuation and phase shift of the 11-year cycle signal in the measured Δ^{14}C (*e.g.* Bard *et al.*, 1997). Because of the attenuation, individual 11-year cycles can hardly be resolved in Δ^{14}C data. The existing literature contains controversies about the phase and the period of the cyclic behavior of Δ^{14}C during the Maunder Minimum: some studies (Peristykh and Damon, 1998; Usoskin, Mursula, and Kovaltsov, 2001) suggest that there is a dominant 22-year cycle with a subdominant 11-year one, while other studies (Miyahara *et al.*, 2004) report a dominant $\approx$ 16-year cyclicity. On the other hand, ^{10}Be data depict the Schwabe cycles (likely somewhat stretched; see Fligge, Solanki, and Beer, 1999) during the Maunder Minimum with the amplitude being comparable to that during the recent high cycles (Beer, Tobias, and Weiss, 1998; Berggren *et al.*, 2009). It was shown that the 11-year cycle in the ^{10}Be data may be out of phase with sunspot numbers (Usoskin, Mursula, and Kovaltsov, 2001), contrary to the normal anti-phase relation, although the reason is unclear. For example, Owens, Usoskin, and Lockwood (2012) and Wang and Sheeley (2013) speculate that it might be due to the changing role of different mechanisms forming the heliospheric magnetic flux. Here we focus on the fact that the amplitude of the cycle in ^{10}Be and ^{14}C during the Maunder Minimum is comparable to those during the recent high-activity cycles (see Figures 1 and 2), without discussing the phase.

This study is in response to an argument that the observed strong cosmogenic-isotope variability would be in contradiction with the weak solar/heliospheric activity during the Maunder Minimum, as, *e.g.*, stated by Svalgaard (2013) "a vigorous solar-cycle modulation of the cosmic-ray flux is observed (*e.g.* Berggren *et al.*, 2009, Figure 10) indicating to this author that significant solar magnetic field was present [during the Maunder Minimum]". Here we analyze the relation between the amplitude of the 11-year cycle observed in the cosmogenic isotopes and solar magnetic activity and show that indeed a significant cosmic-ray modulation is expected even for a grand minimum of solar activity because of the nonlinearity of the relation between sunspot numbers and cosmic-ray flux.

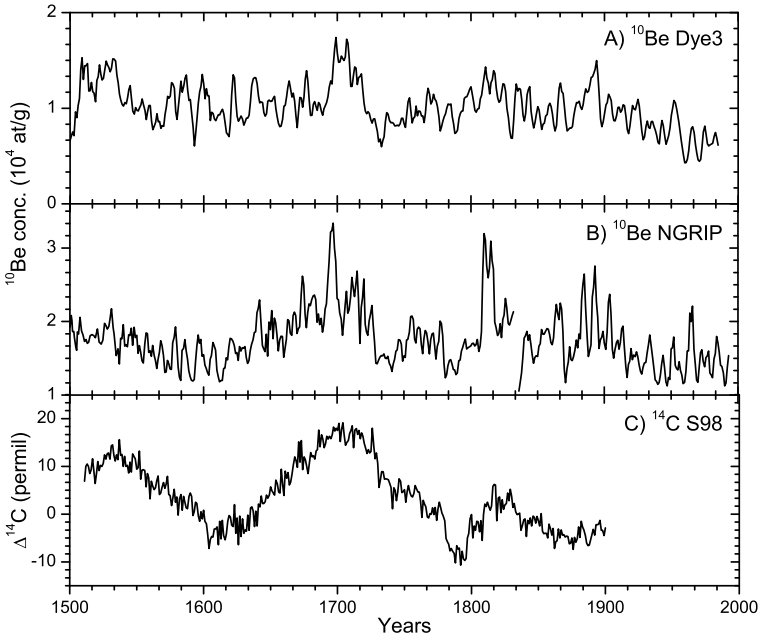

Figure 1 Measured concentrations of ^{10}Be in polar ice cores. All data are three-point running averages. A) Quasi-annual ^{10}Be concentration in the Dye-3 ice core (Beer *et al.*, 1990). B) Quasi-annual ^{10}Be concentration in the NRGIP series (Berggren *et al.*, 2009). C) Annual Δ^{14}C data (Stuiver and Braziunas, 1993; Stuiver, Reimer, and Braziunas, 1998).

2. Method

We model the cosmic-ray modulation and the isotope production and transport for two scenarios: the MM-scenario, corresponding to the conditions of the Maunder Minimum; and the HA-scenario, corresponding to the very high activity observed during the Modern Grand Maximum (Solanki *et al.*, 2004).

2.1. Modern High-Activity Period (HA-Scenario)

The modern period corresponds to unusually high sunspot activity, the Grand Maximum (Solanki *et al.*, 2004), taking place since the 1950s until 2009. However, the current Solar Cycle 24 is moderate, corresponding to the regular sunspot-activity level (*e.g.* Gibson *et al.*, 2011) as, for example in the 19th century. Sunspot-cycle variability was high during the Grand Maximum with the smoothed sunspot number reaching 200 during the maximum phase of Cycle 19. The modulation parameter ϕ is calculated from the data of the ground-based neutron-monitor network, and it varies in a cyclic manner between 400 and 1000 MV (Usoskin, Bazilevskaya, and Kovaltsov, 2011). Throughout this article ϕ is used as defined by Usoskin *et al.* (2005). The reduction of other definitions to this one is discussed elsewhere (Usoskin *et al.*, 2005; Herbst *et al.*, 2010) The geomagnetic field during the modern epoch is moderate with the geomagnetic dipole moment being $M \approx 7.8 \times 10^{22}$ A m^2 (IGRF: www.ngdc.noaa.gov/IAGA/vmod/igrf.html).

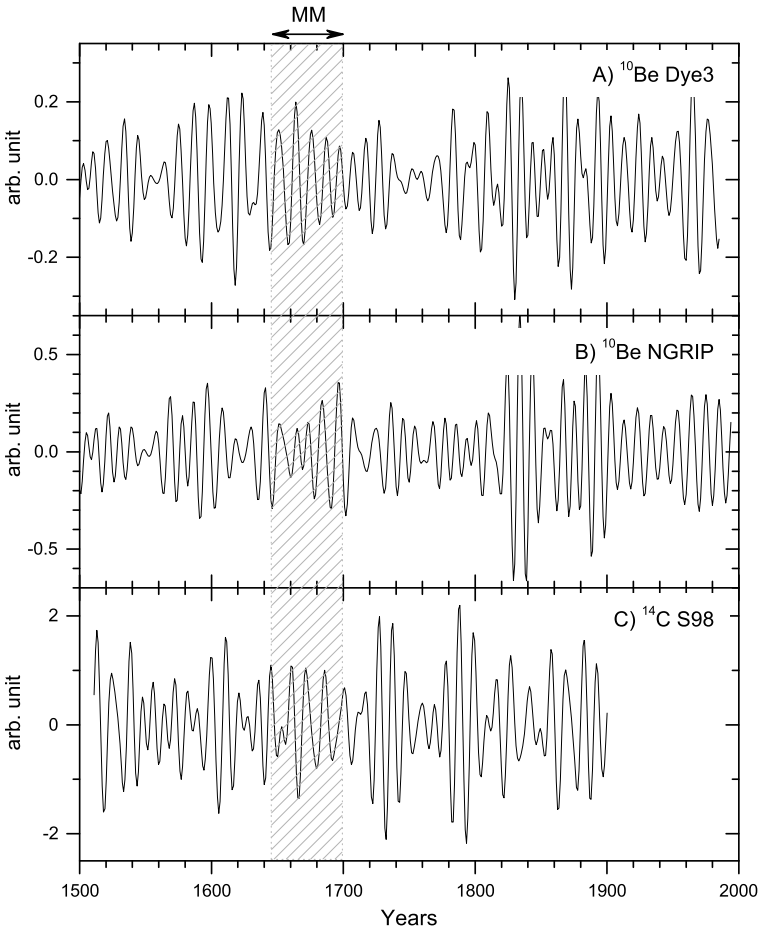

Figure 2 Band-pass filtered (8 – 15 years FFT band-pass filter with rectangular window) of data shown in Figure 1. The vertical hatched area denotes the Maunder Minimum 1645 – 1700.

2.2. Maunder Minimum (MM-Scenario)

The Maunder Minimum was the period of greatly reduced sunspot activity that took place in 1645 – 1715 (Eddy, 1976). Sunspots almost completely vanished (Ribes and Nesme-Ribes, 1993; Hoyt and Schatten, 1996, 1998; Hathaway, 2010). The heliospheric magnetic activity was also greatly reduced. The average heliospheric magnetic field was estimated to be as low as ≤ 2 nT (McCracken, 2007), *cf.* 7 nT during the recent cycles, and the open solar magnetic flux was below 2×10^{14} Wb, *cf.* 7×10^{14} Wb for the recent cycles (Solanki, Schüssler, and Fligge, 2002; Owens, Usoskin, and Lockwood, 2012). On the other hand, the 11-year cycle was clear in heliospheric and geomagnetic indices.

The heliospheric modulation of cosmic rays was weak but still present during the Maunder Minimum. According to different estimates, the mean level of the modulation parameter ϕ, which quantifies the cosmic-ray modulation (Vainio *et al.*, 2009), was between 0 and 300 MV (McCracken *et al.*, 2004; Vonmoos, Beer, and Muscheler, 2006; Muscheler *et al.*, 2007; Usoskin, Solanki, and Kovaltsov, 2007; Steinhilber *et al.*, 2012).

Here we assumed that the mean value of ϕ was ≈ 160 MV during a grand minimum (Usoskin, Solanki, and Kovaltsov, 2007) with the amplitude (half-magnitude) of the 11-year cyclic variation of 100 MV. Although this choice is somewhat arbitrary, we note that it is consistent with an estimate of a purely theoretical model (see Figure 1 of Owens, Usoskin, and Lockwood, 2012). Thus, for the MM-scenario, we consider the cyclically variable ϕ from 60 to 260 MV (see Figure 3a). We also note that the geomagnetic field was stronger during the Maunder Minimum than today, with the magnetic dipole moment $[M]$ being about $(9.15 \pm 0.2) \times 10^{22}$ A m^2 (Licht *et al.*, 2013).

Data of cosmogenic ^{10}Be with annual resolution measured in the Greenland Dye-3 and NGRIP ice cores (see Figure 1) depict the essential 11-year variability during the Maunder Minimum (Beer, Tobias, and Weiss, 1998; Berggren *et al.*, 2009). The amplitude of the cycles appears comparable to that during the modern high cycles (see Figure 2a and b). While the 11-year cycle is nearly seen in the raw Δ^{14}C data (Figure 1c), band-pass-filtered data depict a notable cyclic variability during the Maunder Minimum (Figure 2c). This does not agree with our earlier conclusion (Usoskin, Mursula, and Kovaltsov, 2001) about the dominant 22-year variability of Δ^{14}C during the Maunder Minimum. However, the earlier conclusion was based on another ^{14}C data series of Kocharov *et al.* (1995), which is prone to large systematic uncertainties (Damon, Eastoe, and Mikheeva, 1999). This may explain the difference, which is not, however, relevant for this study.

Thus, the cosmogenic-isotope data suggest (Figure 2) that the amplitude of the 11-year cycle in cosmic rays during the Maunder Minimum was comparable with that of the modern epoch contrary to naive expectations, while the solar/heliospheric conditions were much quieter.

2.3. 11-Year Cycle Variability

Next we calculated the expected signal in the cosmogenic isotopes for the two scenarios considered above. The signal propagation from the input (the modulation parameter) to output (the cosmogenic-isotope production) is shown in Figure 3. We note that, while production of ^{10}Be is usually considered as directly related to the measured concentration/flux in ice cores, it is more complicated for ^{14}C. The ^{14}C production rate is related to the measured Δ^{14}C via the global carbon cycle, which attenuates and delays the production signal (*e.g.* Bard *et al.*, 1997). Thus, the calculated production rate of ^{14}C is not the same as the measured signal. The input, *i.e.* the 11-year cycle in the modulation parameter ϕ, for the two scenarios is shown in Figure 3a. The cycle amplitude is a factor of three greater for the HA-scenario (300 MV) than for the MM-scenario (100 MV), and the cycle-mean level is different by a factor of 4.4 (700 *vs.* 160 MV, respectively).

First we computed the global mean production of ^{14}C using the recent production model (Kovaltsov, Mishev, and Usoskin, 2012), as shown in Figure 3b. The expected ^{14}C production is shown in panel c. The global carbon cycle is not considered here. Eye-guiding gray lines help in understanding how the model works. One can see that the mean overall level of ^{14}C is a factor 1.35 higher for the MM-scenario (2.3 atom cm^{-2} s^{-1}) than for the HA-scenario (1.7 atom cm^{-2} s^{-1}). On the other hand, the amplitude of the 11-year cycle is for the MM-scenario (0.23 atom cm^{-2} s^{-1}) is 0.7 of that for the HA-scenario (0.33 atom cm^{-2} s^{-1}). Direct comparison with the ^{14}C production rates is problematic because of the cycle attenuation and anthropogenic effects (fossil-fuel burning and nuclear-bomb tests) in the 20th century (Roth and Joos, 2013).

A similar analysis of the deposition of ^{10}Be in Greenland, performed using a recent ^{10}Be production model (Kovaltsov and Usoskin, 2010) and transport/ deposition model (Table 3 of Heikkilä, Beer, and Feichter, 2009), is shown in panels d and e of Figure 3. The

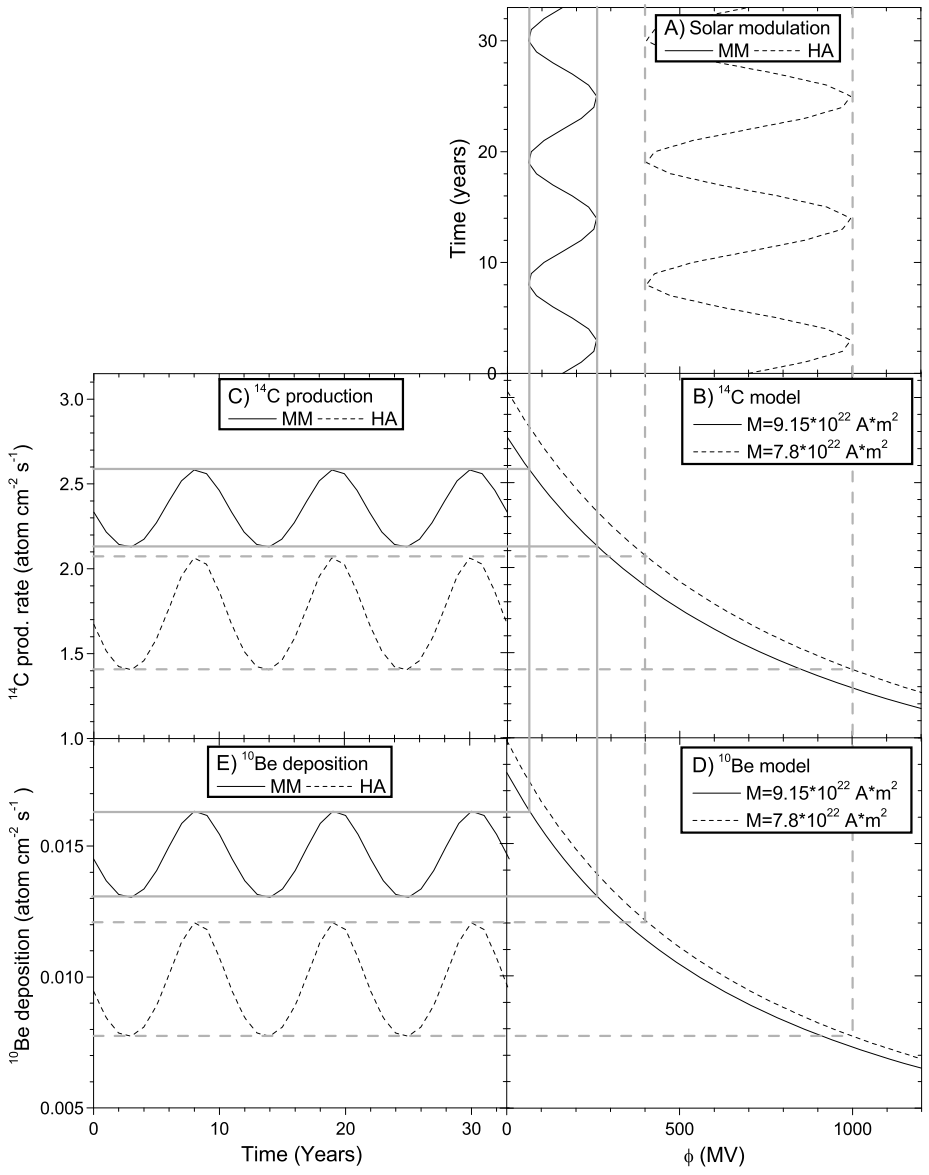

Figure 3 Propagation of the 11-year signal through the cosmogenic-isotope production/deposition model for the MM- (solid lines) and HA- (dashed lines) scenarios. The gray lines (solid and dashed for the MM- and HA-scenarios, respectively) are eye-guiding to illustrate the signal propagation. A) 11-year cycles in solar modulation as an input for the model (MM-scenario, $\phi = 60-260$ MV; HA-scenario, $\phi = 400-1000$ MV). B) Dependence of the global ^{14}C production rate on the modulation parameter for a fixed geomagnetic field. The two curves correspond to the Maunder Minimum (the dipole magnetic moment $M = 9.15 \times 10^{22}$ A m^2, solid curve) and the modern epoch ($M = 7.8 \times 10^{22}$ A m^2, dashed curve), respectively. C) The modeled global ^{14}C production rate for the two scenarios. D) The same as panel C but for the Greenland deposition of ^{10}Be using the beryllium transport model (Heikkilä, Beer, and Feichter, 2009; Heikkilä *et al.*, 2013) for the Maunder Minimum and modern epochs, respectively. E) The modeled ^{10}Be deposition in Greenland for the two scenarios.

mean level of ^{10}Be in Greenland ice is higher by a factor of 1.55 for the MM-scenario (0.021 atom cm^{-2} s^{-2}) than for the HA-scenario (0.0135 atom cm^{-2} s^{-2}). Amplitudes of the 11-year cycle are comparable for the MM- (0.0025 atom cm^{-2} s^{-1}, *i.e.* 12 %) and HA-scenarios (0.0031 atom cm^{-2} s^{-1}), with their ratio being 0.8. We note that this variability, computed within the adopted scenario, is totally consistent with the ^{10}Be data measured in different ice cores (Dye3, NGRIP, South Pole) for the Maunder and Spörer Minima: the mean level of ^{10}Be during the minima was 1.6 – 1.7 of that for the HA-period, and the amplitude of the 11-cycle during the grand minima was $\approx$15 % (Webber and Higbie, 2003; McCracken *et al.*, 2004; McCracken, 2004; Berggren *et al.*, 2009). Exact comparison is difficult because of uncertainties related to ^{10}Be transport and deposition (see the discussion by, *e.g.* McCracken, 2004). Since our adopted MM-scenario is consistent with a theoretical model prediction (Owens, Usoskin, and Lockwood, 2012), this suggests that the whole chain works reasonably well.

A similar result can be obtained using other cosmogenic-isotope production models. For example, the ratio of the 11-year cycle amplitudes for MM- and HA-scenarios is 0.7 using the ^{14}C production model by Masarik and Beer (2009), and 0.7 – 0.95 for ^{10}Be using the production model by Webber and Higbie (2003) depending on the atmospheric-mixing model (McCracken, 2004), which is totally consistent with our results above.

We have checked that the ratio between the 11-year cycle amplitudes for the MM- and HA-scenarios is almost independent of the geomagnetic field within a reasonable range of M values between 6×10^{22} and 12×10^{22} A m^2, being 0.85 and 0.82 for ^{10}Be and ^{14}C, respectively.

3. Discussion and Conclusions

When comparing the Maunder Minimum (MM) and high-activity (HA) scenarios, we observe that the difference between them is greatest in sunspot numbers, with the 11-year cycle amplitude changing from no spots for MM to 150 – 200 for the HA-scenario, and the mean sunspot number changing from about one to 100. The difference between the scenarios observed in the galactic cosmic-ray modulation parameter is still large, being a factor of 4.4 in the mean level and a factor of three in the 11-year cycle amplitude. However, when these largely different signals are converted into the production rate of cosmogenic isotopes, the difference becomes much smaller. In particular, the amplitude of the 11-year cycle is comparable for both scenarios (within 20 – 30 %), in contrast to dramatic changes in the sunspot number or cosmic-ray modulation. This is a result of the strong nonlinearity of the relation between the sunspot activity and cosmic-ray modulation (see, *e.g.*, Solanki *et al.*, 2004) on one hand, and the modulation parameter and cosmogenic-isotope production, on the other (see panels b and d in Figure 3). The nonlinearity is related, in particular, to the fact that the greater the modulation potential is, the higher is the effective energy of cosmic rays, leading, due to the declining energy spectrum of galactic cosmic rays, to lesser variability of the cosmic-ray flux. We note that this has been discussed by experts in the field (*e.g.* McCracken and Beer, 2014) and implicitly follows from earlier studies (O'Brien, 1979; Castagnoli and Lal, 1980; Lal, 1988; Masarik and Beer, 1999; Webber and Higbie, 2003), but it may not have been widely appreciated leading to an incorrect conclusion that the high cycle amplitude during a grand minimum should indicate high heliospheric magnetic fields (Svalgaard, 2013).

Our model computations of the 11-year cycle in ^{10}Be during the Maunder Minimum are in good agreement with the measured data and suggest that the 11-year variability of the

heliospheric parameters was still significant ($\phi \approx 160 \pm 100$ MV) during the grand minimum and could not be much smaller than that. On the other hand, such a variability cannot be evidence of a strong heliospheric magnetic field during that period, since the overall level of cosmogenic isotopes, both ^{14}C and ^{10}Be, was high. Our results are also in agreement with a purely theoretical model of Owens, Usoskin, and Lockwood (2012) suggesting that the model yields a realistic result.

In summary, cosmic rays (via the cosmogenic-isotope proxy) may exhibit a normal 11-year cycle even when the Sun itself shows hardly any sunspot cycle. This makes the cosmogenic proxy a useful tool to study the solar cycle during the period of grand minima of solar activity.

Acknowledgements G.K. acknowledges partial support from the Program No. 22 of Presidium RAS. Support by the Academy of Finland to the ReSoLVE Center of Excellence (project no. 272157) is acknowledged.

References

Bard, E., Raisbeck, G.M., Yiou, F., Jouzel, J.: 1997, *Earth Planet. Sci. Lett.* **150**, 453. DOI.
Beer, J., McCracken, K., von Steiger, R.: 2012, *Cosmogenic Radionuclides: Theory and Applications in the Terrestrial and Space Environments*, Springer, Berlin.
Beer, J., Tobias, S., Weiss, N.: 1998, *Solar Phys.* **181**, 237. DOI.
Beer, J., Blinov, A., Bonani, G., Hofmann, H.J., Finkel, R.C.: 1990, *Nature* **347**, 164. DOI.
Berggren, A.-M., Beer, J., Possnert, G., Aldahan, A., Kubik, P., Christl, M., Johnsen, S.J., Abreu, J., Vinther, B.M.: 2009, *Geophys. Res. Lett.* **36**, L11801.
Castagnoli, G., Lal, D.: 1980, *Radiocarbon* **22**, 133.
Cliver, E.W., Boriakoff, V., Bounar, K.H.: 1998, *Geophys. Res. Lett.* **25**, 897. DOI.
Damon, P.E., Eastoe, C.J., Mikheeva, I.B.: 1999, *Radiocarbon* **41**(1), 47.
Eddy, J.A.: 1976, *Science* **192**, 1189.
Fligge, M., Solanki, S.K., Beer, J.: 1999, *Astron. Astrophys.* **346**, 313.
Gibson, S.E., de Toma, G., Emery, B., Riley, P., Zhao, L., Elsworth, Y., Leamon, R.J., Lei, J., McIntosh, S., Mewaldt, R.A., Thompson, B.J., Webb, D.: 2011, *Solar Phys.* **274**, 5. DOI.
Hathaway, D.H.: 2010, *Living Rev. Solar Phys.* **7**, 1. DOI.
Heikkilä, U., Beer, J., Feichter, J.: 2009, *Atmos. Chem. Phys.* **9**, 515.
Heikkilä, U., Beer, J., Abreu, J.A., Steinhilber, F.: 2013, *Space Sci. Rev.* **176**, 321. DOI.
Herbst, K., Kopp, A., Heber, B., Steinhilber, F., Fichtner, H., Scherer, K., Matthiä, D.: 2010, *J. Geophys. Res.* **115**, D00I20. DOI.
Hoyt, D.V., Schatten, K.: 1996, *Solar Phys.* **165**, 181. DOI.
Hoyt, D.V., Schatten, K.: 1998, *Solar Phys.* **179**, 189. DOI.
Kocharov, G.E., Ostryakov, V.M., Peristykh, A.N., Vasil'ev, V.A.: 1995, *Solar Phys.* **159**, 381. DOI.
Kovaltsov, G.A., Mishev, A., Usoskin, I.G.: 2012, *Earth Planet. Sci. Lett.* **337**, 114.
Kovaltsov, G.A., Usoskin, I.G.: 2010, *Earth Planet. Sci. Lett.* **291**, 182. DOI.
Lal, D.: 1988, Solar-terrestrial relationships and the Earth environment in the last millennia. In: Cini Castagnoli, G. (ed.) *Proceedings of the International School of Physics "Enrico Fermi", Course XCV*, North-Holland, Amsterdam, 216.
Licht, A., Hulot, G., Gallet, Y., Thébault, E.: 2013, *Phys. Earth Planet. Inter.* **224**, 38. DOI.
Masarik, J., Beer, J.: 1999, *J. Geophys. Res.* **104**, 12099.
Masarik, J., Beer, J.: 2009, *J. Geophys. Res.* **114**, D11103. DOI.
McCracken, K.G.: 2007, *J. Geophys. Res.* **112**(A11), A09106. DOI.
McCracken, K.G.: 2004, *J. Geophys. Res.* **109**(A18). DOI.
McCracken, K.G., Beer, J.: 2014, *J. Geophys. Res.* **119**, 2379. DOI.
McCracken, K.G., McDonald, F.B., Beer, J., Raisbeck, G., Yiou, F.: 2004, *J. Geophys. Res.* **109**(A18), 12103. DOI.
Miyahara, H., Masuda, K., Muraki, Y., Furuzawa, H., Menjo, H., Nakamura, T.: 2004, *Solar Phys.* **224**, 317. DOI.
Muscheler, R., Joos, F., Beer, J., Müller, S.A., Vonmoos, M., Snowball, I.: 2007, *Quat. Sci. Rev.* **26**, 82. DOI.
O'Brien, K.: 1979, *J. Geophys. Res.* **84**, 423.
Owens, M.J., Usoskin, I., Lockwood, M.: 2012, *Geophys. Res. Lett.* **39**, L19102. DOI.

Peristykh, A.N., Damon, P.E.: 1998, *Solar Phys.* **177**, 343. DOI.
Ribes, J.C., Nesme-Ribes, E.: 1993, *Astron. Astrophys.* **276**, 549.
Roth, R., Joos, F.: 2013, *Clim. Past* **9**, 1879. DOI.
Solanki, S.K., Schüssler, M., Fligge, M.: 2002, *Astron. Astrophys.* **383**, 706. DOI.
Solanki, S.K., Usoskin, I.G., Kromer, B., Schüssler, M., Beer, J.: 2004, *Nature* **431**, 1084. DOI.
Steinhilber, F., Abreu, J.A., Beer, J., Brunner, I., Christl, M., Fischer, H., Heikkilae, U., Kubik, P.W., Mann, M., McCracken, K.G., Miller, H., Miyahara, H., Oerter, H., Wilhelms, F.: 2012, *Proc. Natl. Acad. Sci. USA* **109**(16), 5967. DOI.
Stuiver, M., Braziunas, T.F.: 1993, *Holocene* **3**, 289.
Stuiver, M., Reimer, P.J., Braziunas, T.F.: 1998, *Radiocarbon* **40**, 1127.
Svalgaard, L.: 2013, *J. Space Weather Space Clim.* **3**, A24. DOI.
Usoskin, I.G.: 2013, *Living Rev. Solar Phys.* **10**, 1. DOI.
Usoskin, I.G., Bazilevskaya, G.A., Kovaltsov, G.A.: 2011, *J. Geophys. Res.* **116**, A02104. DOI.
Usoskin, I.G., Mursula, K., Kovaltsov, G.A.: 2001, *J. Geophys. Res.* **106**, 16039. DOI.
Usoskin, I.G., Solanki, S.K., Kovaltsov, G.A.: 2007, *Astron. Astrophys.* **471**, 301. DOI.
Usoskin, I.G., Alanko-Huotari, K., Kovaltsov, G.A., Mursula, K.: 2005, *J. Geophys. Res.* **110**. DOI.
Vainio, R., Desorgher, L., Heynderickx, D., Storini, M., Flückiger, E., Horne, R.B., Kovaltsov, G.A., Kudela, K., Laurenza, M., McKenna-Lawlor, S., Rothkaehl, H., Usoskin, I.G.: 2009, *Space Sci. Rev.* **147**, 187. DOI.
Vonmoos, M., Beer, J., Muscheler, R.: 2006, *J. Geophys. Res.* **111**(A10), A10105. DOI.
Wang, Y., Sheeley, N. Jr.: 2013, *Astrophys. J.* **764**(1), 90.
Webber, W.R., Higbie, P.R.: 2003, *J. Geophys. Res.* **108**, 1355. DOI.